VII International Conference on Computational Methods in Marine Engineering
MARINE 2017
M. Visonneau, P. Queutey and D. Le Touzé (Eds)

NUMERICAL PREDICTION FOR MANY FLOATING DEBRIS TRANSPORTED IN CITY MODEL DUE TO TSUNAMI-INDUCED FLOWS

S. USHIJIMA*, D. TORIU*, K. AOKI, H. ITADA† and D. YAGYU‡**

* ACCMS, Kyoto University, Sakyou-ku, Kyoto-city, 606-8501, Japan
e-mail: ushijima.satoru.3c@kyoto-u.ac.jp

** IHI Corporation, 1-1, Toyosu 3, Koto-ku, Tokyo, 135-8710, Japan

† Mitsui O.S.K. Lines, Ltd., 1-1 Toranomon 2-chome, Minato-ku, Tokyo, 105-8688, Japan

‡ CERE, Kyoto University, Katsura, Kyoto-city, 615-8540, Japan

Key words: Tsunami, Floating Debris, Multiphase Model, Parallel Computation

Abstract. A three-dimensional computational method based on multiphase modelling is employed to predict the behaviors of floating tsunami debris in coastal residential areas. The present computational method enables us to deal with the interactions between free-surface flows and the movements of floating objects, as well as the collisions among the objects and fixed structures. The present method was first applied to simple stability problems of floating cylinders and then it was applied to the 1/250 scale tsunami experiments. Finally, two types of numerical experiments were performed using larger number of floating objects in more complicated conditions. As a result, it was shown that the present method is effective to predict the behaviors of floating objects transported by tsunami between buildings on non-uniform grand surfaces.

1 INTRODUCTION

In the Great East Japan Earthquake in 2011, floating debris transported by tsunami caused serious secondary damage against buildings and other structures in coastal residential areas. Thus, it is important to develop a numerical method to estimate the behaviors and distributions of the floating objects transported by tsunami in coastal regions.

There have been some studies to propose computational methods for solid objects drifting in waves and tsunami as reported by Kawasaki et al. [1], Yoneyama et al. [2] and others. In contrast to the usual methods, a large number of floating objects can be calculated accurately with the present method in more complicated conditions, since it gives us the reasonable solutions for the difficulties to treat the collisions among objects, fluid-solid interactions and computational load to calculate large problems.

In this study, a computational method based on a multiphase modelling (called MICS) [3] is employed and the outline of the governing equations and numerical procedures is shown, in order to calculate floating objects transported by tsunami flows, taking account of the fluid-solid interactions and collisions among the objects and fixed structures.

The basic validity of the present method was first confirmed by applying it to the stability problems of floating cylinders. Then it was applied to the experimental results obtained in a 1/250 scale city model in the flume of DPRI in Kyoto University. As a result of the calculations, it was shown that the predicted distributions of 42 floating objects transported in the city model are in good agreement with the experimental results. On the basis of the above validation, two types of numerical experiments were conducted : (1) 240 truck models transported by dam-break flows with and without debris control structures (DCS) on non-uniform ground surfaces and (2) 156 floating objects drifting in a 1/250 scale city model whose area is larger than the experimental one. As a result of the numerical experiments, it was demonstrated that the present computational method is expected to enable us to propose various prevention measures and effective design against the secondary disaster caused by tsunami debris.

2 NUMERICAL PROCEDURES

2.1 Multiphase model and basic equations

In the numerical prediction of tsunami debris, it is necessary to use the advanced computational method that enables us to calculate three-dimensional free-surface flows and fluid-solid interactions as well as the collisions among solid objects. For that purpose, three-dimensional parallel computation method (MICS) [3], which has been proposed on the basis of the multiphase model, is employed in this study. Figure 1 (a) illustrates the multiphase field, consisting of gas, liquid and solid phases, in a computational cell. The present model was derived by assuming that all phases are incompressible and immiscible with the averaging procedures for multiple phases [4]. The governing equations for gas-liquid phase consist of the incompressible condition and equations for mass and momentum conservations, which are given as follows :

$$\frac{\partial u_i}{\partial x_i} = 0 \tag{1}$$

$$\frac{\partial \rho_f}{\partial t} + \frac{\partial (\rho_f u_i)}{\partial x_i} = 0 \tag{2}$$

$$\frac{\partial u_i}{\partial t} + \frac{\partial (u_i u_j)}{\partial x_j} = -\frac{1}{\rho_f}\frac{\partial p}{\partial x_i} + g_i + \frac{1}{\rho_f}\frac{\partial}{\partial x_j}\left[\mu\left(\frac{\partial u_i}{\partial x_j} + \frac{\partial u_j}{\partial x_i}\right)\right] \tag{3}$$

where t is time, x_i is the component of the orthogonal coordinate system and g_i is the x_i component of the external acceleration. While u_i is the mass-averaged velocity of gas and liquid phases, the volume-averaged variables are used for pressure p, density ρ_f and coefficient of viscosity μ.

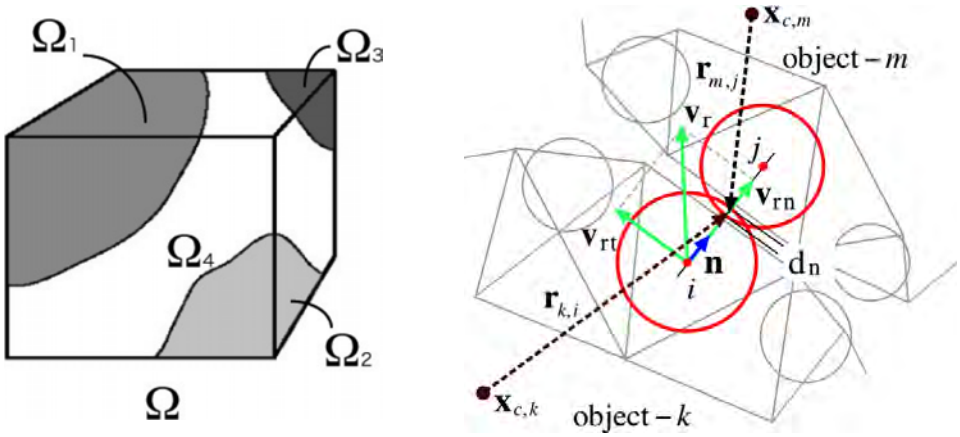

(a) Multiphase field in cell Ω (Ω_k : volume of $k-$phase)

(b) Contact of two objects

Figure 1: Multiphase field and solid object model

2.2 Outline of numerical procedures

Equations (1), (2) and (3) are discretized with a finite volume method on the collocated grid system, which is a structured Eulerian grid system. In contrast, the solid objects are represented by multiple tetrahedron elements as schematically shown in Fig. 1 (b), whose node points are treated in a Lagrangian way on the Eulerian grid system used for gas and liquid phases.

The numerical solutions for gas and liquid phases are calculated with the modified SMAC method from the original one [6], in which an implicit discretization technique, a C-ISMAC method [7], is applied to reduce elapsed time for computations in addition to easily implement the fifth-order TVD scheme [8] for convection terms in Eqs. (2) and (3). In the calculations of a pressure field, a C-HSMAC method [3] is employed to satisfy incompressible condition. As a result of the C-HSMAC method, the discretized velocity components defined on cell boundaries, which are used to calculate fluxes in the finite volume method, satisfy accurately the incompressible condition given by Eq. (1).

In addition, in an attempt to reduce the elapsed time of computation, the present method is completely parallelized with flat MPI (Message-Passing Interface) [9] on the basis of a three-dimensional domain decomposition method.

2.3 Calculations of floating objects

The floating objects transported by tsunami flows are assumed to be rigid bodies which have no deformation due to the collision with the other objects, while the contact forces between objects are estimated using multiple contact-detection spheres set up within the solid model as shown in Fig. 1 (b). The normal and tangential forces arising in the contact are calculated on the basis of a distinct element method (DEM) [10].

The movements of the floating objects are calculated with the basic equations for translational

and rotational motions. The basic equation of the translational motion is given by

$$M_b \dot{\boldsymbol{v}} = \boldsymbol{F}_F + \boldsymbol{F}_C \tag{4}$$

where M_b is the mass of an object, $\boldsymbol{v}$ is the velocity vector of its center and dot means time differentiation. On the right hand side of Eq. (4), both fluid force $\boldsymbol{F}_F$ and contact force $\boldsymbol{F}_C$ are taken into account. The basic equation of the rotational motion, Euler equation, is given by

$$\dot{\boldsymbol{\omega}} = \boldsymbol{I}^{-1}\left[R^{-1}\boldsymbol{N} - \boldsymbol{\omega} \times \boldsymbol{I}\boldsymbol{\omega}\right] \tag{5}$$

where $\boldsymbol{\omega}$ is the angular velocity vector, $\boldsymbol{I}$ is inertia tensor in the basic attitude of the object, R is a rotation matrix and $\boldsymbol{N}$ is the external torque resulting from $\boldsymbol{F}_F$ and $\boldsymbol{F}_C$. The calculation related to the rotation is actually performed with quaternion instead of the multiplication of the rotation matrix R. The location and attitude of the floating object are determined form Eqs.(4) and (5). The x_i component of the fluid force f_{Fi}, which acts on a part of an object included in one cell, is calculated with the pressure and viscous terms of Eq. (3) :

$$f_{Fi} = \Delta m \left[-\frac{\rho_b - \rho_f}{\rho_b} g \delta_{3i} - \frac{1}{\rho_b}\frac{\partial p}{\partial x_i} + \frac{1}{\rho_b}\frac{\partial}{\partial x_j}\left\{ \mu \left(\frac{\partial u_i}{\partial x_j} + \frac{\partial u_j}{\partial x_i} \right) \right\} \right] \tag{6}$$

where Δm is the mass of the part of the object included in a cell and ρ_b is the volume-average density including solid phase in a cell. Taking x_3 axis vertically upward, g is the acceleration of gravity and δ_{3i} is a Kronecker delta. The summation of f_{Fi} over all cells including the same object corresponds to the component of the fluid force $\boldsymbol{F}_F$ on the right hand side of Eq. (4). The volume fraction of solid phases included in a computational cell, such as Ω_1 illustrated in Fig. 1 (a), is estimated with a sub-cell method [5].

3 VALIDATION OF COMPUTATIONAL METHOD

3.1 Stabilities of floating cylinders

It is important to estimate the stability and attitude accurately in the prediction of floating objects in free-surface flows. As a basic validity, the present method was applied to a simple problem, in which the attitudes of two floating cylinders classified into stable and unstable conditions are calculated with the present computational method. Figure 2 shows the geometry and variables. The specific gravity is 0.5 and the diameter D is 0.1 [m] for both cylinders. The axial lengths L are set as follows : $L = 0.05$ [m] in Cylinder-A (stable) and $L = 0.1$ [m] Cylinder-B (unstable). The stability of the cylinders due to initial disturbance is classified with the plus or minus sign of the following s :

$$s = \frac{I_y}{V_s} - \overline{GB} \tag{7}$$

where G and B are centers of gravity and buoyancy, while V_s is the immersed volume and I_y is the moment of inertia of the shaded area on waterline section, as shown in Fig. 2 (b), around $y-$axis.

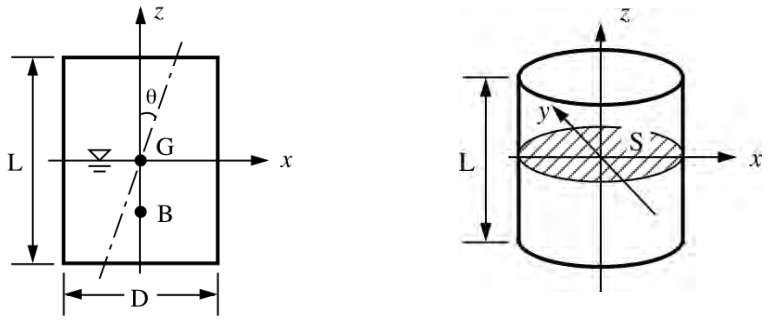

(a) Vertical section of cylinder (b) Coordinates and waterline

Figure 2: Floating cylinder and coordinates

The predicted results of two cylinders are shown in Figs. 3 and 4. The cylinders are represented by tetrahedron elements and the interactions between cylinders and the flows of air and water are also calculated. The initial disturbances θ indicated in Fig. 2 (a) are set at $\pi/6$ for Cylinder-A and $\pi/60$ for Cylinder-B. As shown in Figs. 3 and 4, it was confirmed that Cylinder-A stably returns to the initial attitude, while Cylinder-B is unstable as expected in theory.

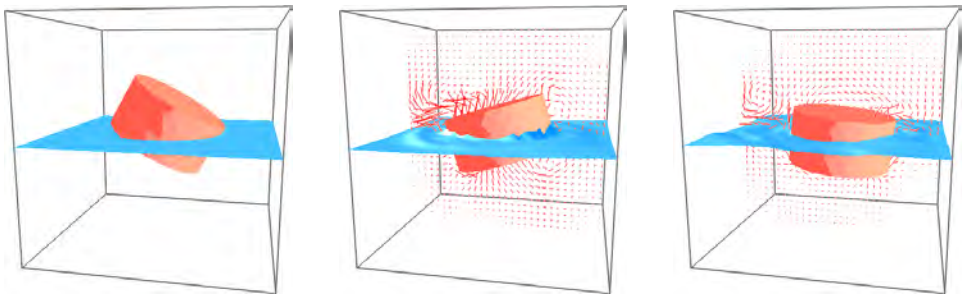

(a) $t = 0.0$ [s] (b) $t = 0.32$ [s] (c) $t = 0.48$ [s]

Figure 3: Calculated results of Cylinder-A (stable, $L/D = 0.5$)

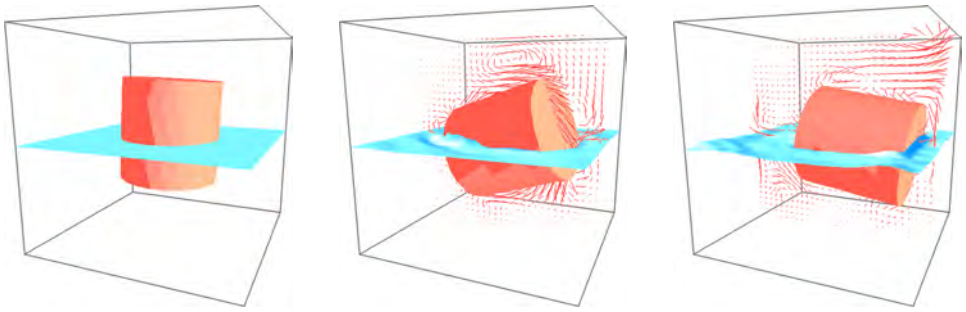

(a) $t = 0.0$ [s] (b) $t = 0.32$ [s] (c) $t = 0.48$ [s]

Figure 4: Calculated results of Cylinder-B (unstable, $L/D = 1.0$)

3.2 Comparisons with tsunami experiments

Hydraulic experiments were conducted using Hybrid Tsunami Open Flume in Ujigawa in DPRI of Kyoto University, in an attempt to measure the transportations and distributions of floating objects in a 1/250 scale city model. Figure 5 (a) shows a schematic view of the flume, while Fig. 5 (b) is a photograph of a part of the city model including calculation area. In experiments, 42 rectangular floating objects, $10 \times 20 \times 10$ [mm] and density 893 [kg/m^3], are placed in front of the city model as shown in Fig. 5 (b). The inflow water of the flow rate 6.7×10^{-2} [m^3/s] was provided during 60 [s], which causes the flows corresponding to actual tsunami about 5 [m] in wave height.

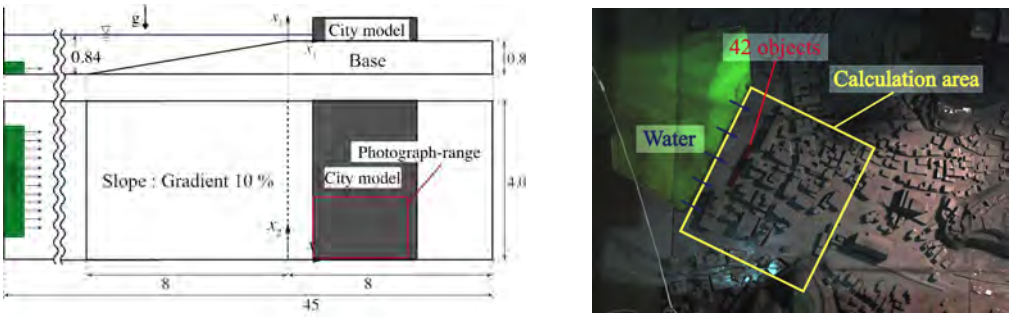

(a) Experimental flume (b) Photograph of city model

Figure 5: Experimental conditions

The computational domain shown in Fig. 6 (a) is a part of the city model as indicated in Fig. 5 (b). The 42 floating objects and main buildings are included in the computational domain, $x_1 \times x_2 = 0.25 \times 0.95$ [m]. Figure 6 (b) shows the details of a computational floating model, which is represented by 134 ($\equiv N_e$) tetrahedron elements and 72 contact detection spheres. The density of the floating model is same as the experimental one. The number of computational cells is $350 \times 270 \times 250$ in $x_1 \times x_2 \times x_3$ directions and 300-parallel computations were executed.

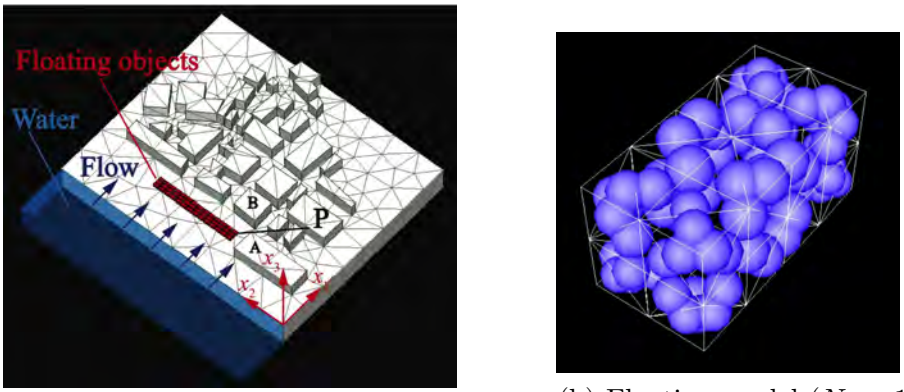

(a) City model for computation (b) Floating model ($N_e = 134$)

Figure 6: Conditions of computations

Figure 7 shows the distributions of the center points of the floating objects, which were measured three times in experiments. It was shown that the floating objects are transported through the wide streets between buildings with the passage of time. The calculated distributions of the floating objects are shown in Fig. 8. In calculations, the floating objects shown in Fig. 6 (b) are transported by the free-surface flows colliding with the other objects and buildings. It was confirmed that the calculated distributions of the objects are almost in good agreement with the experiments from the comparisons between Figs. 7 and 8.

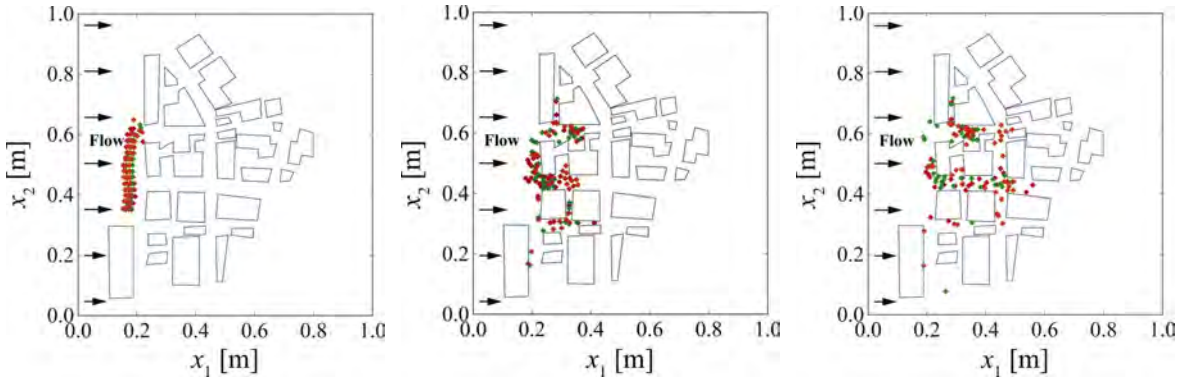

(a) $t = 0.0$ [s] (b) $t = 3.0$ [s] (c) $t = 6.0$ [s]

Figure 7: Experimental results of floating objects transported in city model (3 cases)

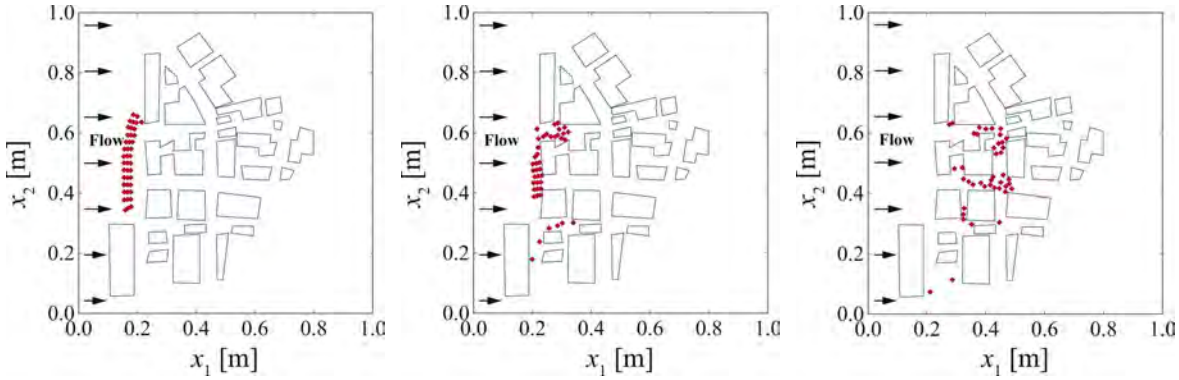

(a) $t = 0.0$ [s] (b) $t = 3.0$ [s] (c) $t = 6.0$ [s]

Figure 8: Calculated results of floating objects transported in city model

4 NUMERICAL EXPERIMENTS

4.1 Floating trucks and debris control structures (DCS)

Numerical experiments were conducted with the present method in order to confirm its applicability to more complicated-shaped floating objects and non-uniform ground surfaces in addition to estimating the effects of debris control structures (DCS) [11].

Figure 9 shows the conditions of calculations, which correspond to a small scale model. As shown in Fig. 9 (a), in a computational domain, $l_1 \times l_2 \times l_3 = 2.0 \times 1.0 \times 0.2$ [m], rectangular water mass is initially placed in the area, where $x_1 \leq 0.3\ l_3$ and $x_3 \leq 0.4\ l_3$, to cause dam-break flow in the domain. Figure 9 (b) shows 240 floating truck models and 10 fixed cylindrical DCS with grand surface which has two hemisphere-like high areas. The diameter of DCS is 90 [mm]. The shape of each truck model is shown in Fig. 9 (c), which is represented by tetrahedron elements, whose number $N_e = 399$, as indicated in Fig. 9 (d) with wire-frames. The densities of DCS and truck models are 3.57×10^2 and 2.56×10^3 [kg/m^3] respectively.

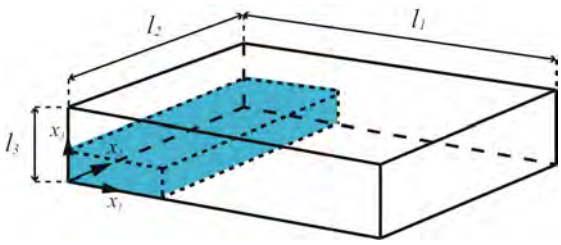

(a) Calculation area and water mass

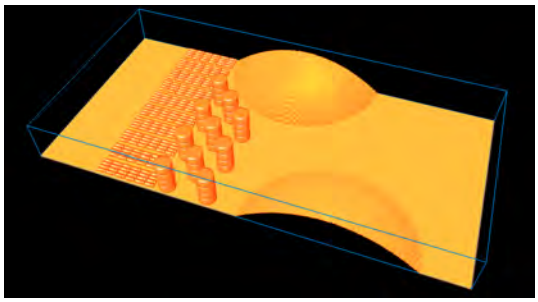

(b) Trucks and DCS on ground surface

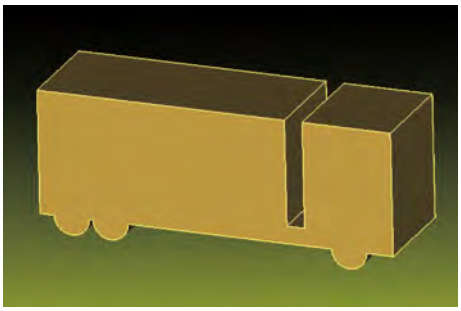

(c) Shape of one truck model

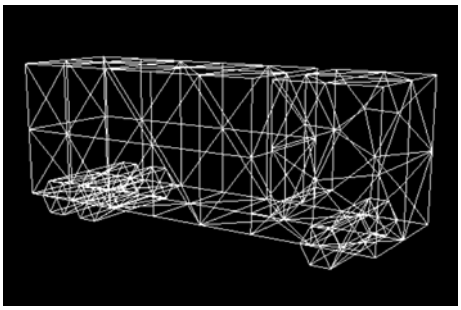

(d) Wire-frame of truck model ($N_e = 399$)

Figure 9: Conditions of numerical experiments with trucks and DCS

In the calculations, the number of computational cells is $400 \times 200 \times 40$, while the domain is decomposed into $20 \times 10 \times 2$ with 400-parallel computations. The time increment Δt is 5.0×10^{-4} [s]. Figures 10 and 11 show the predicted results for two cases of computations : with DCS and without DCS. As shown in Fig. 10, without DCS, it was seen that the truck models are transported far into the downstream area on the lower grand surface due to the free-surface flows. In contrary, as shown in Fig. 11, it was confirmed that most of the truck models are trapped in front of DCS. From the above results, it can be concluded that the present method is expected to provide us with the efficient measures and design methods against the secondary disaster of tsunami, which is caused by many floating objects.

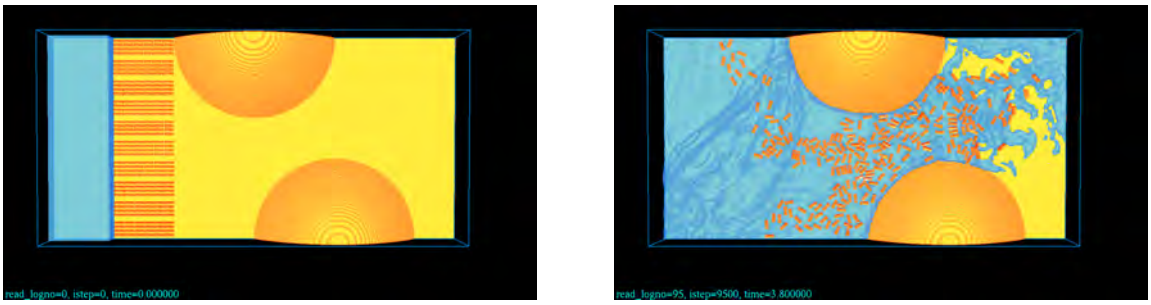

(a) $t = 0$ [s] (b) $t = 3.8$ [s]

Figure 10: Transported truck models without DCS

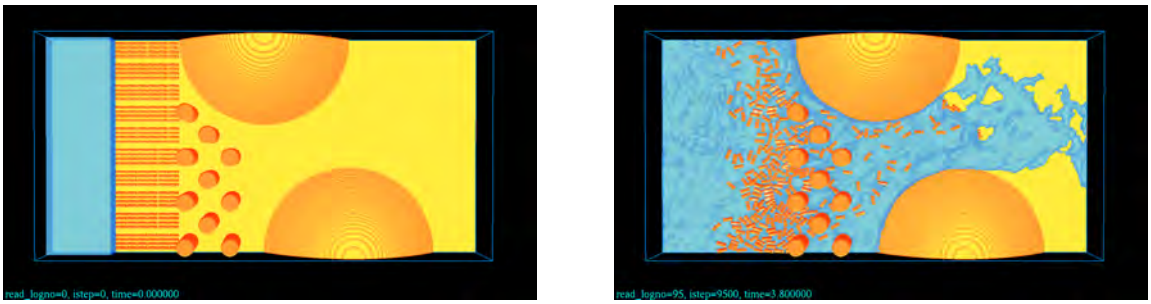

(a) $t = 0$ [s] (b) $t = 3.8$ [s]

Figure 11: Transported truck models with DCS

4.2 Tsunami debris transported in a wide range of city model

Numerical experiments were conducted with a 1/250 scale artificial city model whose area is larger than the experiments described in 3.2, in order to confirm the applicability of the present method to more complicated city model with many floating objects.

Figure 12 (a) shows the conditions of computations. The flow rate from the inlet area is 1.353×10^{-3} [m^3/s]. The 156 floating objects, which assume to be nearly maximum-loading containers, were initially placed in front of the city model as shown in Fig. 12 (b). Their geometry is rectangular $10 \times 20 \times 10$ [mm] and the density is 600 [kg/m^3]. Each floating object is represented by 134 tetrahedron elements and each includes 16 contact-detection spheres.

The number of computational cells was $345 \times 231 \times 64$ and the computational domain in Fig. 12 (a) was decomposed into $15 \times 11 \times 2$ subdomains, to which 330-parallel computation was applied. The total elapsed time was about 59 hours to calculate 24.0 [s] shown in Fig. 12 (d).

As shown in Figs. 12 (b) to (d), the floating objects are transported by the free-surface flows colliding with the other objects and buildings. It is seen that they move through relatively wide spaces between buildings and that the transition of their distributions is reasonably predicted in the flooded regions.

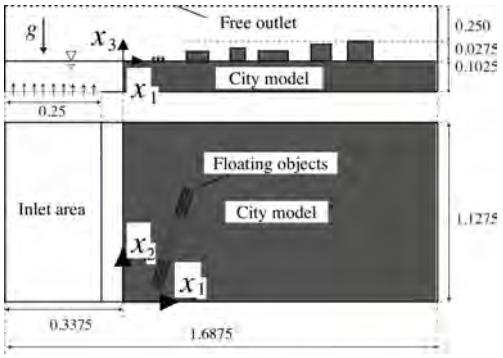

(a) Conditions of computations

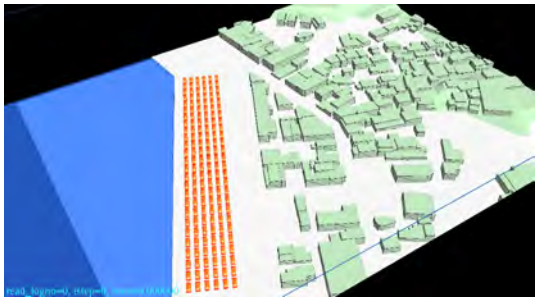

(b) $t = 0.0$ [s]

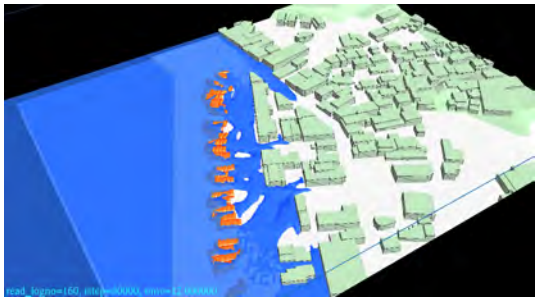

(c) $t = 12.0$ [s]

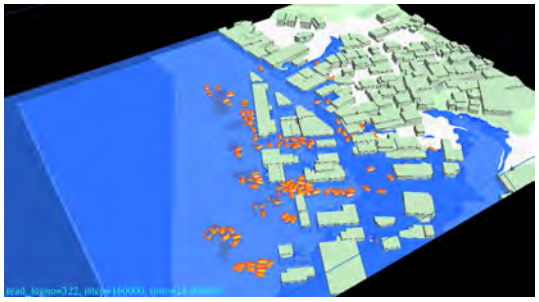

(d) $t = 24.0$ [s]

Figure 12: Conditions of calculations and predicted results

5 CONCLUSIONS

In this study, a computational method based on a multiphase modelling (MICS) [3] was employed and its governing equations and numerical procedures were shown in order to calculate the floating objects transported by tsunami flows taking account of the fluid-solid interactions and collisions among many objects and fixed structures.

The basic validity of the present method was first confirmed by applying it to the stability problems of floating cylinders. Then it was applied to the experimental results obtained in a 1/250 scale city model in the flume of DPRI in Kyoto University. As a result of calculations, it was shown that the predicted distributions of 42 floating objects transported in the city model are in good agreement with the experimental results. On the basis of the above validation, two types of numerical experiments were conducted : (1) 240 truck models transported by dam-break flows with and without debris control structures (DCS) on non-uniform ground surfaces and (2) 156 floating objects in a 1/250 scale city model whose area is larger than the experimental one. As a result of the numerical experiments, it was demonstrated that the present computational method is expected to enable us to propose various prevention measures and design against the secondary disaster of tsunami.

ACKNOWLEDGEMENTS

The experiments in DPRI were supported by Prof. N. Yoneyama and Prof. N. Mori in Kyoto University. The authors would like to thank them for their contribution to this study.

REFERENCES

[1] K. Kawasaki, S. Yamaguchi, M. Hakamada, N. Mizutani, and S. Miyajima. Wave pressure acting on drifting body after collision with bore. *Ann. J. Coast. Eng., JSCE*, 53:786–790, (2006).

[2] N. Yoneyama, H. Nagashima, and K. Toda. Three-dimensional numerical analysis to predict behavior of driftage carried by tsunami. *Earth Planets Space*, 64:965–972, (2012).

[3] S. Ushijima. Multiphase-model approach to predict arbitrarily-shaped objects moving in free surface flows. *Proc of APCOM'07 – EPMESC XI*, MS41–3–1, (2007).

[4] D. A. Drew and S. L. Passman. *Theory of Multicomponent Fluids*. Springer, (1999).

[5] S. Ushijima and N. Kuroda. Multiphase modeling to predict finite deformations of elastic objects in free surface flows. *Fluid Structure Interaction V, WIT Press*, 34–45, (2009).

[6] A. A. Amsden and F. H. Harlow. A simplified MAC technique for incompressible fluid flow calculations. *J. Comp. Phys.*, 6:322–325, (1970).

[7] S. Ushijima and I. Nezu. Higher-order implicit (C-ISMAC) method for incompressible flows with collocated grid system. *JSCE Journal*, (719/II-61):21–30, (2002).

[8] S. Yamamoto and H. Daiguji. Higher-order-accurate upwind schemes for solving the compressible Euler and Navier-Stokes equations. *Computers Fluids*, 22(2/3):259–270, (1993).

[9] W. Gropp, E. Lusk, and R. Thakur. *Using MPI-2*. The MIT Press, (1999).

[10] P. A. Cundall and O. D. L. Strack. A discrete numerical model for granular assemblies. *Geotechnique*, 29(1):47–65, (1979).

[11] K. Aoki, S. Ushijima, H. Itada, and D. Toriu. Parallel computations for many floating objects transported by tsunami flows. *PANACM2015, Buenos Aires, Argentina*, 611–622, (2015).